Strong-field photoionization of O_2 at intermediate light intensity

Tomasz Kłoda,[1] Akitaka Matsuda,[2] Hans O. Karlsson,[3] Mohamed Elshakre,[4] Per Linusson,[1] John H. D. Eland,[5] Raimund Feifel,[6] and Tony Hansson[1,*]

[1]*Department of Physics, Stockholm University, AlbaNova University Center, SE-106 91 Stockholm, Sweden*
[2]*Institute for Molecular Science, National Institute of Natural Sciences, Myodaiji, Okazaki, Aichi 444-8585, Japan*
[3]*Department of Physical and Analytical Chemistry, Quantum Chemistry, Uppsala University, Box 518, SE-751 20 Uppsala, Sweden*
[4]*Department of Chemistry, Cairo University, 126 13 Cairo, Egypt*
[5]*Department of Chemistry, Physical and Theoretical Chemistry Laboratory, Oxford University, South Parks Road, Oxford OX1 3QZ, United Kingdom*
[6]*Department of Physics and Astronomy, Uppsala University, Box 516, SE-751 20 Uppsala, Sweden*

(Received 5 July 2010; published 27 September 2010)

We investigated by electron spectroscopy the strong-field multiphoton ionization of O_2 molecules with ultrashort laser pulses in the intensity range between the multiphoton and tunneling regimes. The ionization proceeds by at least three different mechanisms, in addition to the eight- and nine-photon nonresonant pathways. Transient multiphoton resonances with vibrational Rydberg levels give rise to direct Freeman-type peaks with sublaser linewidth and spin-orbit splitting. Some resonance levels actually become populated and yield extremely narrow lines because of postpulse vibrational autoionization. When the lowest photon order resonance channel for the Rydberg states is closed, a third contribution becomes dominant with a main peak at 0.4 eV that shares its main properties with the recently discovered universal low-energy structure in the electron spectra of atoms and molecules [C. I. Blaga *et al.*, Nat. Phys. **5**, 335 (2009); W. Quan *et al.*, Phys. Rev. Lett. **103**, 093001 (2009)]. The variation of the Freeman resonance spectrum with the laser peak intensity is well correlated with the vibronic Franck-Condon factors for the overlap of the intermediate Rydberg state with the O_2 ground state. Accordingly, the Freeman peaks could be unambiguously assigned to individual vibronic multiphoton resonances, and the disappearance of the Freeman resonances at a certain laser intensity could be explained. The population of the autoionizing Rydberg states could be assigned similarly to such vibronic resonances.

DOI: 10.1103/PhysRevA.82.033431 PACS number(s): 33.80.Rv, 42.50.Hz

I. INTRODUCTION

The present frontier research in attosecond phenomena [1,2] fuels a considerable effort in the scientific community to improve our understanding of the behavior of atoms and molecules in intense electromagnetic fields. The pertinent fields are strong enough to significantly modify the forces governing the evolution of the unperturbed systems, and a pivotal process in this context is field-induced ionization. Given the magnitude of typical atomic and molecular valence electron forces, a lower limit on the strong field range can be defined at 1 TW/cm^2. At these intensities, multiphoton processes leading to ionization are important, and effects like multiorder above threshold ionization (ATI) [3], manifested by photoelectrons carrying away multiples of the photon energy, and ac Stark shifts of Rydberg states leading to Freeman resonances in ionization appear [4]. Much of the current research concerns intensities above about 100 TW/cm^2, for which direct tunneling dominates the ionization process and high-order harmonics generation becomes operative [5–8].

In general, the strong-field processes are considered to be well understood for atoms (see [9] for a recent review). Important effects are still being discovered, though. It was very recently found that the low-energy spectrum of the photoelectrons from atoms and molecules exhibits a universal structure [10,11]. It occurs for field wavelengths of 800 nm or longer in an intensity range that is intermediate between the multiphoton and tunneling regimes. This low-energy structure (LES) in the photoelectron spectrum appears to have no generally accepted explanation yet, but it may be related to the Coulomb interaction between the outgoing electron and its parent ion [11].

In comparison to the case of atoms, the understanding of the strong-field ionization of molecules is fairly limited [12,13]. The major complication, of course, is the additional degrees of freedom associated with nuclear motion, which makes the full quantum mechanical theoretical treatment still a most challenging problem even for the simple neutral hydrogen molecule [14]. Photoelectron spectroscopy in the subtunneling intensity regime indicates that Freeman-type resonances with Rydberg states as well as higher valence states play a crucial role also for molecules [15–19]. As for atoms, such Rydberg resonances appear in the electron spectrum as sharp peaks located at E_γ-E_b, where E_γ is the photon energy and E_b is the electronic binding energy of the Rydberg state, independent of the light intensity [16,17,19]. Particular molecular phenomena that occur because of the inherent atomic multicenter nature, in addition to alignment and orientation effects [20–22], include molecular bond softening and hardening, enhanced ionization, above-threshold dissociation, and Coulomb explosion [12]. Nuclear dynamics can also influence the electron emission greatly [18,23]. Major attention has been paid to the total ion yield as a function of field intensity compared to atoms with similar ionization potentials. The general behavior is the same for the same ionization potential irrespective of the nature of the system.

*tony.hansson@fysik.su.se

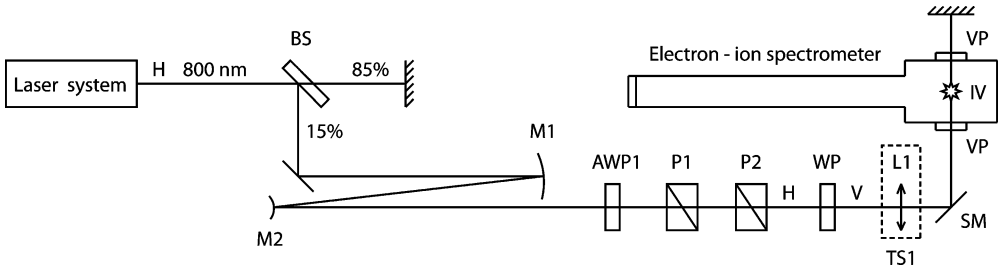

FIG. 1. Schematic of the experiment setup. Legend: H (V), horizontal (vertical) polarized beam; BS, beam splitter; M1, M2, concave-convex mirror telescope; AWP1, adjustable half-wave plate; P1, P2, thin-film polarizers; WP, half-wave plate; L1, focusing lens; TS1, translation stage; SM, steering mirror; VP, viewport; IV, interaction volume.

A few exceptions have been found, however, among those O_2 in which molecular systems exhibit a suppressed ionization rate [24–28]. This has been attributed to interference between parts of the outgoing electron wavefunction that may occur in open-shell systems [29–36]. The ionization suppression in oxygen molecules is the same for linear and circular polarization, which has been taken as evidence that Freeman resonances are unimportant for strong-field ionization of this molecule [27].

Apart from the extensive work on the ionization suppression phenomenon and the related multielectron ionization [24,37–48] occurring in the tunneling ionization regime, there exist only a few published studies of the strong-field ionization of the O_2 molecule. References [23] and [49] investigated ionization mechanisms in the multiphoton ATI regime with visible and ultraviolet laser pulses of 0.5 ps to 10 ns duration. In this intensity and duration range, an intricate interplay between various parallel resonant and nonresonant pathways is observed. Reference [50] employed shorter visible and near-infrared pulses to study the plasma formation in oxygen gas. They could distinguish different ionization regimes and concluded that multiphoton ATI dominates for wavelengths of 405 nm and laser peak intensities $\lesssim$12 TW/cm^2, whereas tunneling ionization occurs for 810 nm light and 35 TW/cm^2.

In the present article, we present high-resolution photoelectron spectra obtained in strong-field ionization of O_2 with 800 nm pulses of about 45 fs duration in the intensity range intermediate between the multiphoton and the tunneling ATI regimes. Our electron spectra reveal strong Freeman resonances with sublaser linewidths that are split by spin-orbit interaction in the final ionic state. These unexpected features are discussed by us in a separate article [51], where we show that they are related to a line shape that is basically Lorentzian, with a corresponding effective decay time by ionization of the O_2 molecules much shorter than the laser pulse duration and the period of the spin-orbit interaction, as well. Here we analyze the electron spectrum and its laser intensity dependence over the whole low-energy range, including the first two ATI structures. In addition to the aforementioned Freeman resonances, we also observed long-lived vibrationally autoionizing states and a low-energy structure with similar properties to the recently discovered universal LES feature [10,11]. Guided by model calculations, we assign the Freeman peaks to individual vibronic Rydberg resonances and infer that the autoionizing states are populated via similar resonances.

II. EXPERIMENT

A schematic of the experimental setup is shown in Fig. 1. The overall system consists of an amplified femtosecond laser coupled to a high-resolution magnetic bottle electron time-of-flight spectrometer with multiparticle coincidence detection capability [52]. The electron spectrometer optionally could be combined with an ion time-of-flight mass spectrometer akin to the setup used in [53,54].

The data presented here were acquired with the 800 nm output from the amplified Ti:sapphire femtosecond laser system (Coherent Legend USP-HE). The laser pulses from this system had a duration of 40–50 fs and integrated energy of 2.1 mJ at 1 kHz repetition rate. A 15% fraction of the laser beam was split off, reduced twofold in beam diameter, and further variably attenuated in a wave plate–polarizer combination with fixed final linear polarization. The laser pulses were focused with a spherical planoconvex lens with a focal length of 35 cm into the interaction volume of the electron spectrometer with the polarization perpendicular to the electron spectrometer time-of-flight axis. The laser pulse duration was expectedly minimized by adjustment of the compressor in the chirped-pulse amplifier to obtain maximal Xe ion yield for a given laser fluence low enough to ensure a substantial contribution from nonresonant ionization pathways. Complementary pulse time–bandwidth characterization was performed with a frequency-resolved optical gating device (Newport UPM-8-20). The resulting laser peak intensity in the interaction volume, I_0, was estimated from the ponderomotive shift of the nonresonant ionization peak for Xe [55].

The electron spectrometer has been described before [52]. Briefly, it is a 5.5-m-long magnetic bottle electron time-of-flight spectrometer possessing an energy resolution of less than 5 meV for electron kinetic energies below 1 eV and $E/\Delta E$ of 100 or better at electron energies above that. The electron spectrometer could optionally be equipped with an ion time-of-flight mass spectrometer and operated in electron-ion coincidence mode with a mass resolution of about 200 and somewhat reduced electron energy resolution (cf. [53,54]). The ion mass spectra under the present conditions showed no or negligible traces of O^+ formation, except at the very lowest I_0 of 4 TW/cm^2, for which the atomic ion peak height was about 10% of the molecular one. The electron spectra presented here were therefore all taken in the higher-resolution pure electron spectrometer configuration.

The electron spectra were calibrated against known autoionization peaks and energy levels for Xe atoms [56–58] with an absolute energy accuracy of about 5 meV at low energies. Correspondingly, a systematic error of ±2.5 meV has been included in all error estimates referring to determined absolute electron energies. To complete the characterization of the laser-electron spectrometer combination, we note that the nonresonant eight-photon ionization of Xe at relatively low laser intensities yields a peak with 0.12 eV full width at half maximum (FWHM), which is consistent with our laser bandwidth and a $\sqrt{N}$ scaling with the multiphoton order N.

The oxygen gas was let into the interaction region of the spectrometer via a gas needle. The partial oxygen pressure in the chamber was adjusted within the range 3×10^{-8}–8×10^{-5} mbar to accommodate the maximally allowed total count rate of five per laser pulse at the electron detector. At laser peak intensities up to 10 TW/cm^2, the background counts from the 2×10^{-7} mbar residual gas were negligible. Above that limit, background electron spectra were taken in direct connection with the measurement and subtracted from the spectra obtained with O_2 present. The upper laser peak intensity in our measurements was limited to 30 TW/cm^2 by ionization of the residual gas becoming prohibitively large.

III. RESULTS

An overview of electron spectra from singly ionized O_2 at representative laser peak intensities is given in Fig. 2. All spectra exhibit multiple ATI structures separated by the photon energy of 1.55 eV that extend well beyond the displayed range. At the lowest and medium laser peak intensities, we see sharp fine structures in the range 0.9–1.5 eV (B in Fig. 2). They are also seen in the next ATI order with similar relative intensity distribution. At the highest laser intensity, they are gone, and instead, a broad peak at 0.4 eV (C in Fig. 2) is seen, which is also repeated in the next ATI order. Finally, there is, in the low-laser intensity spectrum, a series of very sharp lines superposed on a strong background at the lowest electron energies (A in Fig. 2), which are seen neither in the other two spectra nor in the higher order ATI peaks of this spectrum.

All in all, we discern in these overview electron spectra three qualitatively different peak structures. These have some resonant photoionization character as they match neither the energy position nor the width expected for nonresonant ionization. A peak of the latter kind is seen at about 1.5 eV in the lowest I_0 spectrum because of nonresonant nine-photon ionization. In the same spectrum, the tail of the nonresonant eight-photon ionization is responsible for the strong increase of the signal at the very lowest electron kinetic energies. The relative contributions from the nonresonant peaks to the electron spectra at higher laser peak intensities are small and will be mostly ignored in the following discussion.

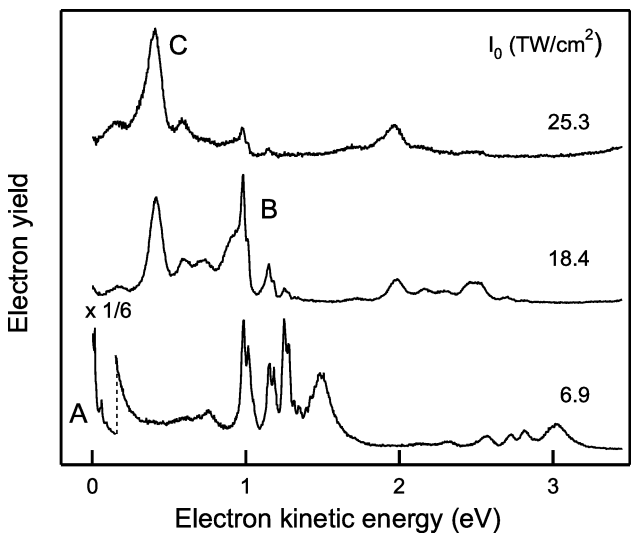

FIG. 2. Representative electron spectra from O_2 covering the first two ATI orders. The spectra were acquired at the indicated laser peak intensities I_0 which, starting from below, correspond to ponderomotive shifts U_p of 0.41, 1.10, and 1.52 eV, respectively. The spectra were normalized to the same maximum peak height, except the low-energy part of the 6.9 TW/cm^2 trace, which was reduced by a factor of 6, and were offset relative to each other for clarity of presentation. A, B, and C refer to spectral structures of different origins, as discussed in the text.

A. Structure A

An expanded view of the low electron energy structure A at laser peak intensities of 6.9 and 9.2 TW/cm^2, respectively, is shown in Fig. 3. Similar structures with very sharp lines on a background are visible in the spectra from the lowest I_0 up to about 12 TW/cm^2. The background changes in this intensity range from a broad peak into a slope rising toward zero electron kinetic energy, as seen in Fig. 3. This evolution

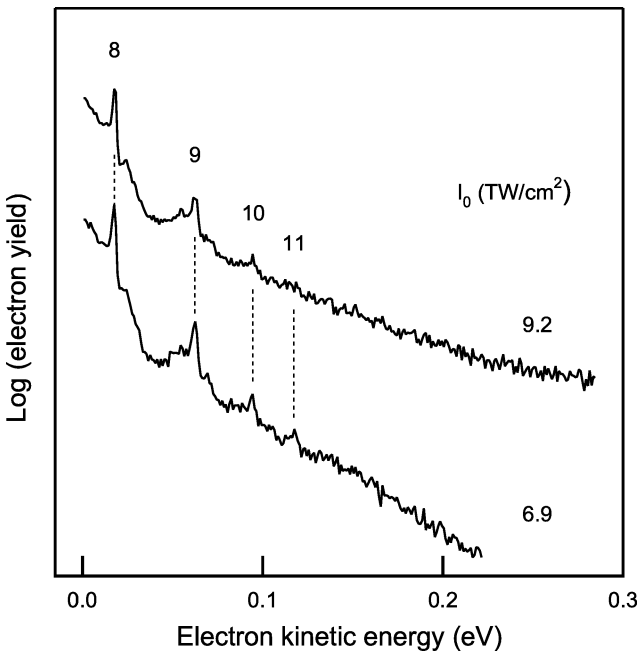

FIG. 3. Electron spectra in the kinetic energy range of structure A in Fig. 2. The spectra were acquired at the indicated laser peak intensities. Our assignments of the peaks marked by vertical lines as owing to vibrational autoionization of Rydberg states are indicated by the effective principal quantum number n. Note the logarithmic scale of the ordinate.

agrees in all parts with the expectations for the nonresonant eight-photon ionization peak [55].

The sharp lines have widths that appear to be limited by our electron spectrometer resolution. Their energy positions are independent of the laser peak intensity, and the absolute count rate in each increases more rapidly than linearly with the laser intensity—a linear log-log fit to the variation of the very lowest energy peak in the two shown spectra together with one for I_0 at 11.5 TW/cm^2 gives a slope of 1.6 ± 0.3 (we use 1 standard deviation error throughout).

The line positions extracted from the electron spectrum obtained for $I_0 = 6.9$ TW/cm^2, for instance, are 0.018, 0.063, 0.095, and 0.117 eV. These compare well to the vibrational autoionization peaks assigned to d Rydberg states with vibrational quantum number $v = 1$ [59], except for an overall negative shift of 6 meV. Thus we assign tentatively the structure A to vibrational autoionization of Rydberg states with effective principal quantum numbers n, as indicated in Fig. 3. Fitting of the four discernible line positions in the figure to the Rydberg formula with a constant quantum defect yields weighted averages for the convergence limit of 230 ± 3 meV and for the quantum defect 0.004 ± 0.002.

B. Structure B

The structure B part of the electron spectrum is shown for a range of laser peak intensities in Fig. 4. The common feature of these spectra is a series of split peaks at fixed energies below E_γ. We have discussed these peaks recently in the context of Freeman-type resonances with Rydberg states, with particular emphasis on the hitherto unobserved line splitting and sublaser linewidth [51]. Here we will focus on the actual assignment of the lines to particular Freeman-Rydberg resonances.

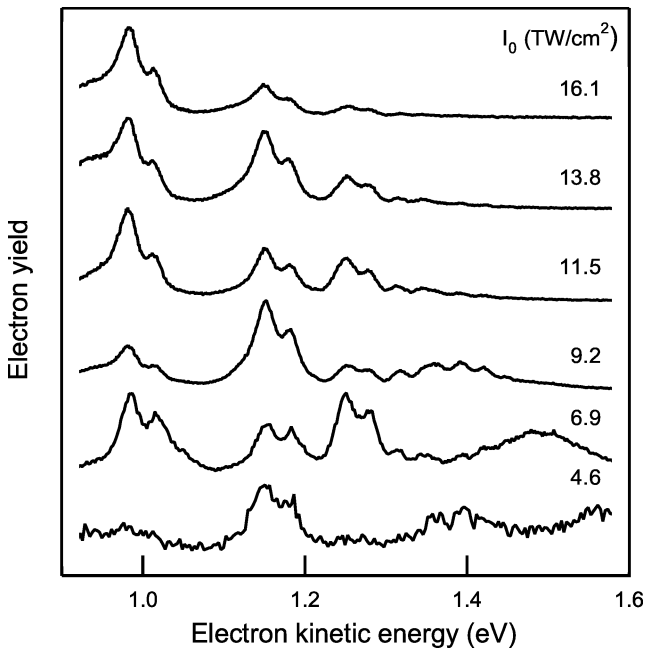

FIG. 4. Electron spectra in the kinetic energy range of structure B in Fig. 2 acquired at the indicated I_0 which, starting from below, correspond to U_p of 0.28, 0.41, 0.55, 0.69, 0.83, and 0.97 eV, respectively. The spectra were normalized to the same maximum peak height and were offset relative to each other for clarity of presentation.

Fits of the peak positions to the Rydberg formula for the 6.9 TW/cm^2 spectrum [51] yield two series that are split by an amount corresponding to the energy difference of the $\Omega^+ = 1/2$ and $3/2$ spin-orbit components of the $O_2{}^+(X\,{}^2\Pi_g)$ electronic ground state. The average of the convergence limits, 1.543 ± 0.003 eV, is close to the photon energy, and the average quantum defect is 0.003 ± 0.007. On these grounds, it was concluded in [51] that the likely physical origin of the peaks is Freeman resonances involving effectively spinless Rydberg electrons that are split by subsequent spin-orbit interaction acting on the photoelectron in the final continuum state.

Freeman resonances are expected to give electron energy peaks at fixed energies irrespective of the laser peak intensity. This is clearly seen in Fig. 4 to be the case for the structure B. The assignment of these peaks in terms of specific Rydberg vibronic resonances, for which the changes in the electron peak amplitudes are instrumental, is discussed in Sec. IV B. In addition to the substantial variation of the relative peak heights, there is a qualitative change between the topmost spectrum in Fig. 4 and the middle one in Fig. 2, despite a rather modest change in laser peak intensity in a range corresponding to a ponderomotive potential $U_p \approx 1$ eV. The structure B is not immediately discernible at laser peak intensities higher than this up to at least 30 TW/cm^2, which is the upper intensity limit for the spectra acquired in this study.

C. Structure C

The structure C comprises at least two broad peaks, a dominating one at 0.41 eV and a smaller one at 0.16 eV. It appears at laser peak intensities of about 14 TW/cm^2 and becomes the main feature of the electron spectrum when the Freeman resonance peaks disappear. It is not explicitly shown here, but the structure C peaks are strongly dependent on the laser polarization and vanish when the light polarization is changed to circular [60]. This stands in contrast to the Freeman peaks, which seem not to change in their appearance with polarization, except for a reduction by about a factor of 2 in the absolute intensity [60]. The structure C peaks remain at fixed energy positions over the whole range of laser peak intensity we used. These energy positions we could not fit to any known O_2 Rydberg levels. Finally, as will be discussed in [60], the peak at 0.75 eV may well belong to this structure as it has similar appearance and laser polarization dependence. It shows, however, a quite different variation with I_0.

IV. DISCUSSION

The laser peak intensities applied here range from 5 to 30 TW/cm^2, which translates into Keldysh parameter values $\sqrt{E_{\mathrm{IP}}/(2U_p)}$ between 5 and 2, where $E_{\mathrm{IP}} = 12.07$ eV is the O_2 ionization potential [61]. Thus we are in an intensity range that is intermediate between the multiphoton and the tunneling ionization regimes [62]. The laser-induced ac Stark shifts of the molecular electronic states are substantial, accordingly. For Rydberg states, these shifts are similar to the ponderomotive

potential U_p of free electrons in the laser field, which here ranges from about 0.3 to 1.8 eV.

The overview electron spectra shown in Fig. 2 were chosen to represent characteristic values of U_p. Thus the lowest trace illustrates the situation when U_p is substantial but still low enough to exhibit vibrational autoionization peaks and a multitude of Freeman-Rydberg resonances. The middle trace corresponds to the highest U_p for which the Freeman-Rydberg resonances constitute a major component of the electron spectrum. When U_p becomes equal to E_γ, a channel closing occurs, and Freeman-Rydberg resonances can only reappear by an increase in the number of photons involved in the fulfillment of the resonance condition. This condition applies to the topmost spectrum of Fig. 2. Clearly almost only the still unassigned structure C is then present.

We will next discuss separately the three qualitatively different structures A, B, and C identified earlier. A general selection rule they share, because of the $^3\Sigma_g^+$ symmetry of the O_2 ground state, is that an even (odd) number of photons interact only with g (u) parity excited states. This puts restrictions on the possible orbital angular momenta of the Rydberg states. The Rydberg series converges to the $O_2{}^+$ ion ground state with $^2\Pi_g$ symmetry, which implies that the overall parity of the Rydberg states is dictated by that of the Rydberg electron: l even (odd) $\leftrightarrow$ g (u). The minimum number of photons required to surpass the 12.07 eV zero-field ionization limit E_{IP} of O_2 is eight. Consequently, we expect in the present data to find only resonances with even-l Rydberg states as we restricted the laser intensities to those for which $U_p < E_\gamma$.

A. Vibrational autoionization

In Sec. III A, we assumed provisionally that the structure A is because of vibrational autoionization of Rydberg states, primarily on the basis of the observed line positions. The Rydberg character of the lines is identified based on the successful fit of their energy positions to a Rydberg series. Their autoionization origin is indicated by the independence of the line positions on I_0 and their extreme narrowness, which facts taken together are only consistent with an ionization process occurring on a much longer time scale than the laser pulse duration. Indeed, similar vibrational autoionization peaks of O_2 were observed by [59] to have linewidths of the order of 0.1 meV.

The vibrational autoionization mechanism is further corroborated by the observed convergence limit of the Rydberg series at 230 ± 3 meV. The total eight-photon angular momentum and energy in the absence of external fields is sufficient to excite the $v = 2$ or lower vibrational states in a range of nl Rydberg states correlating with the two $O_2{}^+(X\,^2\Pi_g)$ spin-orbit components. Thus, because of the $\Delta v = -1$ propensity rule for vibrational autoionization of diatomic molecules [63], we could expect only $v = 1 \rightarrow 0$ and $2 \rightarrow 1$ autoionization transitions to occur with the associated Rydberg series converging to electron energies equaling the corresponding vibrational transition of the ion core. As the two possible ion core states have similar potential energy curves, any Rydberg series built on one of them would exhibit a convergence limit at an electron energy of either 232 or 228 meV [61], in agreement with our fit value.

The quantum defect we extract from the fit to the Rydberg formula is very close to zero. This does not match the value for the d Rydberg states obtained in [59]. More recent measurements on those Rydberg states [64] give a smaller value of the quantum defect with error limits that might be consistent with our value. A more likely explanation, however, could be that some of the Rydberg states which give rise to the Freeman resonances discussed in Sec. IV B actually get populated and remain populated at the end of the laser pulse. These Rydberg states appear to belong to a g series with possible minor contributions from higher l states and have a negligible quantum defect. Later, we will see that the vibronic Freeman resonances corresponding to $v = 1$ for $n \geqslant 8$ are expected to be most intense for laser peak intensities of about 5 TW/cm^2. This correlates well with the spectra in which we see the most well developed autoionization lines. A similar reasoning explains qualitatively the nonexistence of the autoionization peaks at higher laser peak intensities.

It thus seems that structure A originates from vibronic Rydberg levels which are ac Stark shifted in the intense laser field and get populated through multiphoton resonances when the molecules feel an appropriate laser peak intensity, similar to observations in the atomic case [65], and subsequently autoionize vibrationally. This would imply that the autoionizing states are produced primarily in shells of constant laser peak intensity. The signal at I_0 values substantially larger than the minimum required to bring a particular state into resonance, then, should scale as $I_0^{3/2}$ [66]. This is in good agreement with the $I_0^{1.6\pm0.3}$ dependence we find for the $n = 8$ peak amplitude, which is the most well developed one in our data.

B. Molecular Freeman resonances

In a previous article [51], we assigned the structure B to vibronic Freeman resonances with Rydberg states converging to the $O_2{}^+$ electronic ground state. The spin-orbit splitting of the peaks was treated in that context and will not be further discussed here. The same applies to the sublaser linewidth of the peaks, which was observed also for Xe atoms and shown to be related to a decaylike ionization of the Freeman resonance occurring on the time scale of a few tens of femtoseconds. Here we will focus on the assignment of the resonances to particular vibronic Rydberg levels.

As discussed in [51], the spin-orbit interaction in the Rydberg states is too weak to have appreciable influence during the few tens of femtoseconds that it takes to ionize the molecule in the intense laser field, and the peak splitting develops afterward. Therefore one could expect the transient resonances to be well described in terms of spin-free electrons and, as the spin-orbit splitting of the $O_2{}^+\,^2\Pi_g$ ground state is symmetric in energy and the two states have equal statistical weight, take their energies to correspond to the center of the split peaks. This accounts in a natural way for the fact that the convergence limit of the average of the split O_2 Freeman-Rydberg series coincides with that obtained for Xe atoms under comparable conditions. In the following, we will adopt this picture and omit spin-orbit interaction from our analysis and calculations of electron spectra. This will prevent us from reproducing the

Freeman peak splitting, but the relative intensities of peaks belonging to different principal quantum numbers should be reflected.

We begin the vibronic assignment of the Freeman resonances by noting that the Rydberg series contributing to the structure B appears to have only members with $n \geqslant 5$. This indicates that the two lowest n members have angular momentum $l = 4$, which is consistent with the very small quantum defect for the series as well as the $g \leftrightarrow g$ parity selection rule applying to the eight-photon resonance expected to be involved in the process. For the higher n members, also, larger even-l states could participate; however, the corresponding states have increasingly poorer overlap with the ion core region, where the ionization is mostly taking place. This has been found to cause a general propensity for the sharpest atomic Freeman peaks to belong to f and g Rydberg series with essentially no contribution from h or higher [67,68], even though the higher l states can become appreciably populated [67]. Such nonpenetrating states are very similar in atoms and molecules, and we assign on these grounds the observed Freeman peaks as mainly because of a g Rydberg series. In the following, we will denote these states accordingly, with the reservation that for $n \geqslant 7$, some small higher l contributions cannot be rigorously excluded on the present evidence.

To proceed further with the assignment, we employ a model similar in spirit to those used successfully in [17,18], comprising two components: a multiphoton resonance with molecular states that are shifted upward by an amount U_p in the laser field and a concomitant decay into the ionization continuum. The main contribution to the Freeman resonances comes from the central focal volume when the resonance condition is met at the laser peak intensity [69], which warrants a time-independent model. There is a spatial distribution of laser peak intensities, however, which we take into account approximately by summing over a Gaussian distribution of ponderomotive shifts centered on each nominal U_p. In contrast to atomic Freeman resonances, the molecular ones also involve the nuclear degrees of freedom, and the overlap between vibrational states has to be accounted for, whereas the rotation is essentially frozen on the time scale of our laser pulse duration and can be ignored. The multiphoton resonance strength therefore includes both electronic and vibrational [Franck-Condon factors (FCFs)] contributions. The electronic part we bunch together with that for the ionization step into an effective n^{-q} power scaling of the overall signal. Because of the Rydberg character of the resonant state, the vibrational part of the resonance step is taken to be given by the FCFs for the $O_2{}^+(X^+, v^+) \leftarrow O_2(X, v = 0)$ transition. No vibrational factor appears in the ionization step because of the $\Delta v = 0$ propensity rule for photoionization of Rydberg states.

We used the effective width ΔU_p of the spatial U_p distribution and q as globally adjustable parameters. In the calculations accounted for here, $\Delta U_p = 0.06$ eV (FWHM), and a best value $q = 3$ was found by variation in half-integer steps. All other data were obtained from either calculations or experiment. The energy levels and FCFs were calculated for nonrotating molecules with the LEVEL 7.4 software [70], with the molecular parameters from [61]. The Rydberg electron binding energies were calculated from the Rydberg formula

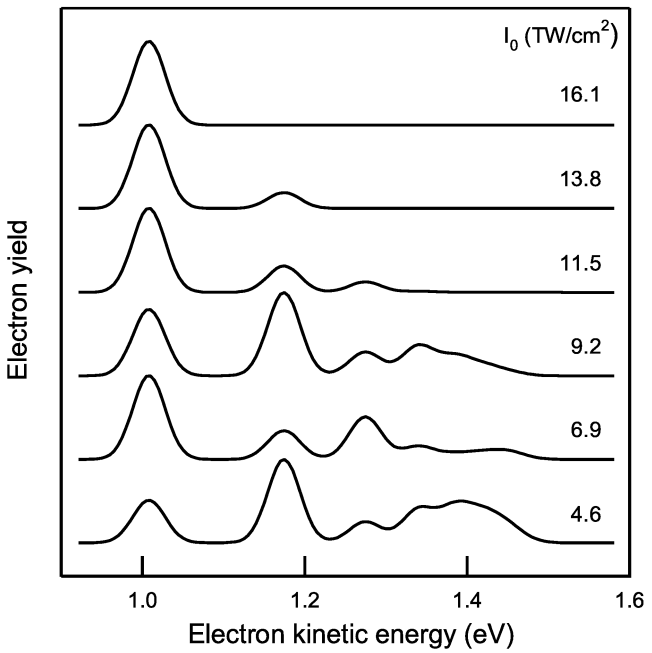

FIG. 5. Calculated electron spectra corresponding to those in Fig. 4. The indicated I_0, starting from below, correspond to U_p of 0.28, 0.41, 0.55, 0.69, 0.83, and 0.97 eV, respectively. The spectra were normalized to the same maximum peak height and were offset relative to each other for clarity of presentation.

without quantum defect. The number of states was restricted to $n \leqslant 12$, and all total angular momentum states were assumed to be identical.

Figure 5 displays electron spectra calculated for a g Rydberg series with zero quantum defect and I_0 values chosen to match those in Fig. 4, to facilitate a direct comparison. The qualitative agreement is remarkably good in view of the simplicity of the model. Of course, the peak splitting is not there in the calculations, but the center electron kinetic energies and the variation of the relative peak heights with I_0 are well reproduced. The origin of the differences is probably found in the use of a time-independent model, the electronic part of the resonance strength, and the crude averaging over the spatial laser intensity. The first two deficiencies require aid from higher level calculations to assess in a meaningful way. The effect of spatial averaging, on the other hand, is well understood [66]. In general, it will contribute components to the electron spectrum that originate from regions with local laser peak intensities less than I_0. This might explain, for instance, the presence of the 1.17 eV peak in the measured spectrum at 16.1 TW/cm^2, while it is not seen in the calculated one.

The fair agreement between the measured and calculated electron spectra in Figs. 4 and 5 confirms our assignment of the peaks as because of Freeman-Rydberg resonances. To elucidate the physical mechanisms behind the variation in relative peak amplitudes, we show in Fig. 6 how the calculated electron spectrum varies with laser peak intensity in more detail. Basically, what is seen for each n state is how its contribution oscillates periodically as the vibrational states go in and out of resonance with changing U_p. The amplitudes of these peaks reflect largely the FCFs for the

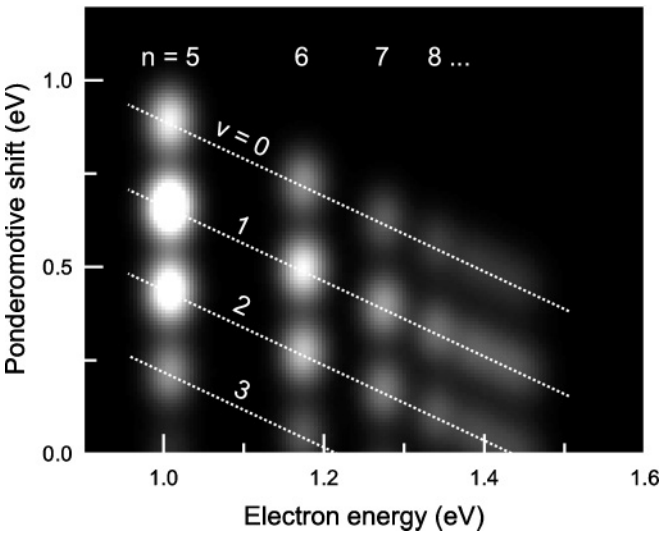

FIG. 6. Overview of the calculated electron spectrum as a function of laser peak intensity reexpressed in terms of U_p. The gray intensity scale is linear from black at zero to white at a cutoff value chosen for clarity of presentation. Assignments of the peaks to vibronic Freeman-Rydberg resonances are indicated. The n numbers apply vertically, while the v numbers run along the diagonal lines.

overlap of the O_2 ground state with the assigned Rydberg vibrational states. There is a maximum ponderomotive shift beyond which a particular n ceases to contribute to the electron spectrum, which occurs when its $v = 0$ level has been shifted above resonance. Thus, at U_p about 1 eV, corresponding to $I_0 \approx 17$ TW/cm^2, the g series of Rydberg states goes through something like a channel closure as above that laser peak intensity, it has shifted completely out of the eight-photon resonance window.

The spectra in Fig. 5 represent horizontal cuts out of Fig. 6. It is now easily seen that the peaks in each spectrum can be assigned to particular vibronic resonances nl_v. The three main peaks in the spectrum at $I_0 = 6.9$ TW/cm^2, for instance, can be identified as $5g_2$, $6g_1$, and $7g_1$. Thus the superficially quite erratic peak amplitude variations in Fig. 4 mainly reflect the variation in vibronic resonance strength, that is, the FCFs for the overlap of the O_2 ground state and the Rydberg states. Figure 6 also provides a clear explanation for the disappearance of the Freeman peaks that sets in between our measured spectra at laser peak intensities of 16.1 and 18.4 TW/cm^2. These embrace precisely the predicted I_0 for the eight-photon channel closure of the g Rydberg series. Furthermore, allowing for the effects of the spatial averaging, we can see clearly in Fig. 4 the sequential closing of individual n vibronic resonance series in accordance with the theoretical predictions: The high-n states at 1.4 eV vanish above $U_p = 0.55$ eV, the $7g_v$ peak decreases as U_p surpasses 0.69 eV, and the $n = 6$ series stops at 0.83 eV so that the $5g_0$ resonance is the last remaining peak at $U_p = 0.97$ eV.

The overall features of the structure B part of the electron spectrum, thus, are readily assignable as Freeman-type resonances with properties analogous to those observed for atoms, as originally suggested by Gibson *et al.* [16] and Helm *et al.* [17]. A general difference to the case of atoms, however, is that the ponderomotive shift U_p required for bringing a particular molecular Rydberg state into resonance is governed by vibronic levels rather than by purely electronic ones. This, we have seen, modulates the relative intensities of the Freeman peaks in accordance with the vibrational overlap of the initial and resonant states. It also allows the molecular Freeman resonances corresponding to a particular n to appear at much smaller U_p than in the case of atoms.

Our identification of Freeman-Rydberg resonances occurring for O_2 is contrary to the conclusions by Wu *et al.* [27] drawn from polarization-dependent total ion yield measurements. Their arguments were based on the assumption that Freeman resonances would not occur at all for circularly polarized light because of angular momentum conservation restrictions in molecules as for atoms [71]. Molecules, however, also have the rotational angular momentum available, and the analogy to atoms seems to be weak in this case. In fact, as is shown in [60], the Freeman resonances observed here remain also for circularly polarized light.

C. Rydberg channel closure and beyond

As described and explained in Sec. IV B, the Freeman-Rydberg resonances disappear rather abruptly at I_0 above about 17 TW/cm^2 because of an eight-photon channel closure. Concomitant with this, structure C becomes the dominant contribution to the electron spectrum. It is strongly dependent on the laser polarization to the extent that it vanishes for circular polarization [60], which is contrary to the behavior of the Freeman resonances. Moreover, we could not match the energy positions of the structure C peaks to any known O_2 Rydberg states.

At present, we have no clear understanding of the structure C other than it has a different origin than the vibronic Freeman resonances seen at lower laser peak intensities. It is tempting, however, as the energy range and polarization dependence are commensurate, to associate it with the recently discovered LES [10,11] observed for both atoms and molecules at somewhat smaller values of the Keldysh parameter than here. The assessment of this association will have to await further theoretical development, as also the LES lacks a fully satisfactory explanation.

Possibly, our peak at 0.75 eV with similar laser polarization dependence is related to the structure C. It has a rather different I_0 dependence, however, and there are a number of other broad peaks in the electron energy range below 1 eV, for instance, the 0.6 eV peak seen in the 18.4 TW/cm^2 spectrum in Fig. 2. The positions of these peaks correlate well with those we obtain in calculations of the time-dependent quantum dynamics for ionization pathways via nine-photon resonances with Rydberg states belonging to excited O_2^+ states. The complexity of the overall dynamics is considerable, however, and we have so far no conclusive assessment of this ionization mechanism.

V. CONCLUSION

The intense-field multiphoton ionization of O_2 molecules with ultrashort laser pulses in the intensity range intermediate between the multiphoton and tunneling regimes proceeds by at least three different mechanisms in addition to the comparably weak eight- and nine-photon nonresonant pathways. Transient

multiphoton resonances with vibronic Rydberg levels give rise to direct Freeman-type peaks with sublaser linewidth and spin-orbit splitting [51] as well as peaks owing to postpulse vibrational autoionization of actually populated levels. When the lowest photon order resonance channel for the Rydberg states is closed, a third contribution becomes dominant, with a main peak at 0.4 eV, that shares its main properties with the recently discovered and still unexplained LES in atomic and molecular electron spectra [10,11].

The Freeman resonance spectrum varies strongly with laser peak intensity. These variations, we showed by comparison to model calculations, depend mainly on the FCFs for the vibrational overlap of the initial O_2 ground state and Rydberg states. Accordingly, the Freeman peaks can be unambiguously assigned to individual vibronic resonances. The vibronic overlap model also successfully predicts the laser peak intensity at which the Freeman resonances disappear in terms of closure of the lowest order photon resonance channel as the vibrational ground level of the lowest lying Rydberg member is shifted above resonance.

The autoionizing states seem to be populated by the same resonance mechanism as the direct Freeman peaks. This accounts well for the observed values of the laser peak intensity at which the autoionization peaks are most prominent and implies that predominantly $v = 1$ levels of Rydberg states with $n \geqslant 8$ are involved.

ACKNOWLEDGMENTS

Our work here has benefited from funding by the Knut and Alice Wallenberg Foundation, the Swedish Research Council (VR), the Swedish Development Agency (Sida/SAREC), and the Swedish Foundation for Cooperation in Research and Higher Education (STINT). We also thank I. Bakken and E. Andersson for their help in setting up the data acquisition system used for the experiments.

[1] P. B. Corkum and F. Krausz, Nat. Phys. **3**, 381 (2007).
[2] F. Krausz and M. Ivanov, Rev. Mod. Phys. **81**, 163 (2009).
[3] P. Agostini, F. Fabre, G. Mainfray, G. Petite, and N. K. Rahman, Phys. Rev. Lett. **42**, 1127 (1979).
[4] R. R. Freeman, P. H. Bucksbaum, H. Milchberg, S. Darack, D. Schumacher, and M. E. Geusic, Phys. Rev. Lett. **59**, 1092 (1987).
[5] W. Becker, F. Grasbon, R. Kopold, D. B. Milosevic, G. G. Paulus, and H. Walther, Adv. At. Mol. Opt. Phys. **48**, 35 (2002).
[6] T. Kanai, S. Minemoto, and H. Sakai, Nature **435**, 470 (2005).
[7] M. Meckel *et al.*, Science **320**, 1478 (2008).
[8] S. Haessler *et al.*, Nat. Phys. **6**, 200 (2010).
[9] P. Agostini and L. F. DiMauro, Contemp. Phys. **49**, 179 (2008).
[10] C. I. Blaga, F. Catoire, P. Colosimo, G. G. Paulus, H. G. Muller, P. Agostini, and L. F. DiMauro, Nat. Phys. **5**, 335 (2009).
[11] W. Quan *et al.*, Phys. Rev. Lett. **103**, 093001 (2009).
[12] J. H. Posthumus, Rep. Prog. Phys. **67**, 623 (2004).
[13] I. V. Hertel and W. Radloff, Rep. Prog. Phys. **69**, 1897 (2006).
[14] Y. V. Vanne and A. Saenz, Phys. Rev. A **80**, 053422 (2009).
[15] S. W. Allendorf and A. Szöke, Phys. Rev. A **44**, 518 (1991).
[16] G. N. Gibson, R. R. Freeman, and T. J. McIlrath, Phys. Rev. Lett. **67**, 1230 (1991).
[17] H. Helm, M. J. Dyer, and H. Bissantz, Phys. Rev. Lett. **67**, 1234 (1991).
[18] J. H. Posthumus, B. Fabre, C. Cornaggia, N. de Ruette, and X. Urbain, Phys. Rev. Lett. **101**, 233004 (2008).
[19] T. Wilbois and H. Helm, Laser Phys. **18**, 579 (2008).
[20] D. Pinkham and R. R. Jones, Phys. Rev. A **72**, 023418 (2005).
[21] D. Pavicic, K. F. Lee, D. M. Rayner, P. B. Corkum, and D. M. Villeneuve, Phys. Rev. Lett. **98**, 243001 (2007).
[22] X. Chu, Phys. Rev. A **78**, 043408 (2008).
[23] B. Walker, M. Saeed, T. Bredeen, B. Yang, and L. F. DiMauro, Phys. Rev. A **44**, 4493 (1991).
[24] C. Guo, M. Li, J. P. Nibarger, and G. N. Gibson, Phys. Rev. A **58**, R4271 (1998).
[25] M. J. DeWitt, E. Wells, and R. R. Jones, Phys. Rev. Lett. **87**, 153001 (2001).
[26] E. Wells, M. J. DeWitt, and R. R. Jones, Phys. Rev. A **66**, 013409 (2002).
[27] J. Wu, H. P. Zeng, and C. L. Guo, Phys. Rev. Lett. **96**, 243002 (2006).
[28] X. H. Ren, J. T. Zhang, P. Liu, Y. Wang, and Z. Z. Xu, Phys. Rev. A **78**, 043411 (2008).
[29] J. Muth-Böhm, A. Becker, and F. H. M. Faisal, Phys. Rev. Lett. **85**, 2280 (2000).
[30] F. Grasbon, G. G. Paulus, S. L. Chin, H. Walther, J. Muth-Böhm, A. Becker, and F. H. M. Faisal, Phys. Rev. A **63**, 041402 (2001).
[31] G. G. Paulus, F. Grasbon, and H. Walther, J. Mod. Opt. **50**, 343 (2003).
[32] A. Jaron-Becker, A. Becker, and F. H. M. Faisal, Phys. Rev. A **69**, 023410 (2004).
[33] V. I. Usachenko and S.-I. Chu, Phys. Rev. A **71**, 063410 (2005).
[34] H. Hetzheim, C. Figueira de Morisson Faria, and W. Becker, Phys. Rev. A **76**, 023418 (2007).
[35] M. Okunishi, K. Shimada, G. Prumper, D. Mathur, and K. Ueda, J. Chem. Phys. **127**, 064310 (2007).
[36] M. Okunishi, R. Itaya, K. Shimada, G. Prumper, K. Ueda, M. Busuladzic, A. Gazibegovic-Busuladzic, D. B. Milosevic, and W. Becker, Phys. Rev. Lett. **103**, 043001 (2009).
[37] A. S. Alnaser, S. Voss, X. M. Tong, C. M. Maharjan, P. Ranitovic, B. Ulrich, T. Osipov, B. Shan, Z. Chang, and C. L. Cocke, Phys. Rev. Lett. **93**, 113003 (2004).
[38] A. S. Alnaser, M. Zamkov, X. M. Tong, C. M. Maharjan, P. Ranitovic, C. L. Cocke, and I. V. Litvinyuk, Phys. Rev. A **72**, 041402 (2005).
[39] C. Cornaggia, J. Lavancier, D. Normand, J. Morellec, P. Agostini, J. P. Chambaret, and A. Antonetti, Phys. Rev. A **44**, 4499 (1991).
[40] E. Eremina, X. Liu, H. Rottke, W. Sandner, M. G. Schatzel, A. Dreischuh, G. G. Paulus, H. Walther, R. Moshammer, and J. Ullrich, Phys. Rev. Lett. **92**, 173001 (2004).
[41] C. L. Guo, M. Li, and G. N. Gibson, Phys. Rev. Lett. **82**, 2492 (1999).
[42] J. Huang, C. Y. Wu, N. Xu, Q. Q. Liang, Z. F. Wu, H. Yang, and Q. H. Gong, J. Phys. Chem. A **110**, 10179 (2006).
[43] D. Normand, C. Cornaggia, J. Lavancier, J. Morellec, and H. X. Liu, Phys. Rev. A **44**, 475 (1991).

[44] L. Quaglia, M. Brewczyk, and C. Cornaggia, Phys. Rev. A **65**, 031404 (2002).
[45] X. M. Tong, Z. X. Zhao, A. S. Alnaser, S. Voss, C. L. Cocke, and C. D. Lin, J. Phys. B **38**, 333 (2005).
[46] S. Voss, A. S. Alnaser, X. M. Tong, C. Maharjan, P. Ranitovic, B. Ulrich, B. Shan, Z. Chang, C. D. Lin, and C. L. Cocke, J. Phys. B **37**, 4239 (2004).
[47] C. Y. Wu, J. Huang, N. Xu, R. Ma, H. Yang, H. B. Jiang, and Q. H. Gong, J. Phys. B **39**, 1035 (2006).
[48] Z. F. Wu, C. Y. Wu, X. R. Liu, Y. Q. Liu, Y. K. Deng, and Q. H. Gong, Opt. Express **18**, 10395 (2010).
[49] B. Bakker, D. Parker, P. Samartzis, and T. Kitsopoulos, J. Chem. Phys. **112**, 5654 (2000).
[50] Z. Mics, F. Kadlec, P. Kuzel, P. Jungwirth, S. Bradforth, and V. Apkarian, J. Chem. Phys. **123**, 104310 (2005).
[51] T. Kloda, M. Elshakre, A. Matsuda, P. Linusson, R. Feifel, and T. Hansson (unpublished).
[52] J. H. D. Eland, O. Vieuxmaire, T. Kinugawa, P. Lablanquie, R. I. Hall, and F. Penent, Phys. Rev. Lett. **90**, 053003 (2003).
[53] J. H. D. Eland and R. Feifel, Chem. Phys. **327**, 85 (2006).
[54] R. Feifel, J. H. D. Eland, L. Storchi, and F. Tarantelli, J. Chem. Phys. **125**, 194318 (2006).
[55] M. D. Perry, O. L. Landen, and A. Szöke, J. Opt. Soc. Am. B **6**, 344 (1989).
[56] S. M. Koeckhoven, W. J. Buma, and C. A. de Lange, Phys. Rev. A **49**, 3322 (1994).
[57] S. M. Koeckhoven, W. J. Buma, and C. A. de Lange, Phys. Rev. A **51**, 1097 (1995).
[58] E. B. Saloman, J. Phys. Chem. Ref. Data **33**, 765 (2004).
[59] S. T. Pratt, J. L. Dehmer, and P. M. Dehmer, J. Chem. Phys. **93**, 3072 (1990).
[60] A. Matsuda *et al.* (unpublished).
[61] R. R. Laher and F. R. Gilmore, J. Phys. Chem. Ref. Data **20**, 685 (1991).
[62] L. V. Keldysh, Sov. Phys. JETP **20**, 1307 (1965).
[63] S. T. Pratt, Annu. Rev. Phys. Chem. **56**, 281 (2005).
[64] H. A. Sheard, T. Ridley, K. P. Lawley, and R. J. Donovan, J. Chem. Phys. **118**, 8781 (2003).
[65] M. P. de Boer and H. G. Muller, Phys. Rev. Lett. **68**, 2747 (1992).
[66] M. D. Perry, O. L. Landen, A. Szöke, and E. M. Campbell, Phys. Rev. A **37**, 747 (1988).
[67] M. P. de Boer, L. D. Noordam, and H. G. Muller, Phys. Rev. A **47**, R45 (1993).
[68] R. M. Potvliege and R. Shakeshaft, Phys. Rev. A **41**, 1609 (1990).
[69] G. N. Gibson, R. R. Freeman, T. J. McIlrath, and H. G. Muller, Phys. Rev. A **49**, 3870 (1994).
[70] R. J. LeRoy, University of Waterloo Chemical Physics Research Report No. CP-642 R^3, 2001 (unpublished).
[71] P. H. Bucksbaum, L. D. van Woerkom, R. R. Freeman, and D. W. Schumacher, Phys. Rev. A **41**, 4119 (1990).